Scientific paper

# Electronic Structures and Reactivities of COVID-19 Drugs: A DFT Study

### Seyda Aydogdu and Arzu Hatipoglu\*

Department of Chemistry, Yildiz Technical University, 34220, Istanbul, Turkey

\* Corresponding author: E-mail: hatiparzu@yahoo.com

Received: 04-06-2022

#### Abstract

These days, the world is facing the threat of pandemic Coronavirus Disease 2019 (COVID-19). Although a vaccine has been found to combat the pandemic, it is essential to find drugs for an effective treatment method against this disease as soon as possible. In this study, electronic and thermodynamic properties, molecular electrostatic potential (MEP) analysis, and frontier molecular orbitals (FMOs) of nine different covid drugs were studied with Density Functional Theory (DFT). In addition, the relationship between the electronic structures of these drugs and their biological effectiveness was examined. All parameters were computed at the B3LYP/6-311++g(d,p) level. The Solvent effect was evaluated using conductor-like polarizable continuum model (CPCM) as the solvation model. It was observed that electrophilic indexes were important to understand the efficiencies of these drugs in COVID-19 disease. Paxlovid, hydroxyquinone, and nitazoxanide were found as the most thermodynamically stable molecules. Thermodynamic parameters also demonstrated that these drugs were more stable in the aqueous media. Global descriptors and the reactivity of these drugs were found to be related. Nitazoxanide molecule exhibited the highest dipole moment. The high dipole moments of drugs can cause hydrophilic interactions that increase their effectiveness in an aqueous solution.

Keywords: COVID-19; SARS-COV-2; Global descriptors; DFT; Solvent effect.

#### 1. Introduction

The Covid-19 outbreak is an important threat to public health nowadays. Many people died, and this pandemic caused a significant economic crisis and panic. During the last few decades, β class of coronaviruses led to mortality diseases like SARS and MERS.1 In December 2019, in Wuhan, China, an outbreak of the new type of Coronavirus Disease (COVID-19) caused a global health and economic crisis. This virus is coronavirus 2 (SARS-COV-2), a type of β coronavirus.<sup>2</sup> Its common symptoms are shortness of breath, fatigue, fever, cough, and flue. In some more severe cases, COVID-19 infection leads to organ failure and even death.3 The mortality rate of COVID-19 is approximately 6.8%, which is smaller than the mortality rate of SARS (10%) and MERS (36%). Despite the smaller mortality rate compared to SARS and MERS, the higher contagious property of COVID-19 and the unpredictability of disease progression worsened the situation and resulted in more deaths worldwide.<sup>1,4,5</sup> To date (January 31.2022), WHO reported that there were 223 countries and territories that suffered from coronavirus with 364,191,494 confirmed cases and death number of 5,631,457 people.<sup>6</sup> Although a vaccine has been found for COVID-19, it is essential to have appropriate drugs that are effective, inexpensive, and easily available for treatment. Therefore, more information is urgently needed on effective drug therapy and possible therapeutics used to combat the COVID-19 pandemic.

It is very difficult to develop a new antiviral drug against COVID-19 and meet the urgent need for treatment. Drug discovery is expensive and time-consuming, a process that takes at least 15 years for a newly designed drug to reach patients from the laboratory.<sup>7,8</sup> These are the limiting factors for control and prevention of this global pandemic.

After analyzing the genome of SARS-COV-2, it is understood that the spike S protein of the virus effectively binds to the human angiotensin-converting enzyme 2 receptors. Once it enters a human cell, it releases immediately and replicates itself. 9,10 Based on this information, many known possible therapeutics have been tested preclinically and clinically so far, but few of them have been proven effective against this disease such as chloroquine, hydroxychloroquine, favipiravir and so on. 11 Remdisevir and chloroquine can be used effectively to cure COVID-19. 12 The

combination of favipiravir with different antiviral agents has been studied for the treatment of COVID-19 and it has been found that the combination of antivirals is an appropriate treatment.<sup>13,14</sup> Nowadays, COVID-19 vaccines are used to prevent the disease. It is also known that at least 54.4% of the world's population receives a dose of vaccine<sup>15</sup>, but drug treatment is still needed to prevent the pandemic.

Computational methods can be a good alternative for studying in such emergency and difficult situations. In comparison to experimental methods, computational ones, are not expensive or time-consuming.<sup>16</sup> There are some studies in the literature by using computational methods related to COVID-19. Molecular docking for inhibition of M<sup>pro,</sup> 3CL<sup>pro</sup>, E proteins, and RdRp enzymes against SARS-COV-2 with drugs such as chloroquine, hydroxychloroquine, favipiravir, umifenovir, paxlovid, galidesivir, ribavirin, molnupiravir, and remdesivir have been investigated. 17-28 Electronic and optoelectronic properties of hydroxychloroquine, chloroquine, azithromycin, and favipiravir were investigated by the DFT method to understand the possible drug delivery system.<sup>29-31</sup> Although many studies have been conducted on the pharmacological properties of COVID-19 drugs, there is still lack of information about the effect of the electronic properties of these molecules on their physicochemical properties and reactivities. Therefore, it is crucial to examine the electronic properties of COVID-19 drugs to better understand their biological effectiveness. As mutations occur in the SARS-COV-2 protein, the need to determine the properties of COVID-19 drugs with rapid and effective methods has become more urgent than ever.

The purpose of this study is to calculate the electronic and thermodynamic properties of already used and newly proposed COVID-19 drugs. DFT method is applied for all calculations. In this respect, some chemical descriptors such as hardness ( $\eta$ ), electrophilic index ( $\omega$ ), chemical potential ( $\mu$ ), softness (S) and frontier orbital energies, and thermodynamic parameters (such as enthalpy, Gibbs free energy, and entropy) are evaluated. Hydroxychloroquine, chloroquine, nitazoxanide, favipiravir, galidesivir, ribavirin, fluvoxamine, molnupiravir and paxlovid are selected as model drugs owing to the differences in their electronic structures. And, their efficiencies are investigated against COVID-19.

## 2. Computational Details

All the calculations were carried out with Density Functional Theory (DFT) method with Gaussian 09 program.<sup>32</sup> The drug molecules were optimized using Becke's three parameter functional which combines Becke and HF exchange with the Lee-Yang-Parr correlation term at B3LYP/6-311++g(d,p) level.<sup>33</sup> Frequency analysis, calculated at the same level of theory, indicated that the opti-

mized structures were at the stationary points corresponding to local minima without any imaginary frequency. The structural visualizations of the drugs were prepared by using the GaussView 5.0 software. Since blood itself is a water-based system, the Conductor-Like Polarizable Continuum Method (CPCM) was used to compute the effect of water on the properties of drugs. The solvent was water with the dielectric constant value  $\varepsilon = 78.3$ . Thermodynamic parameters were obtained by frequency analysis and solvation energies were also calculated. The energies were corrected by including zero-point vibrational energy (ZPVE) at the B3LYP/6-311++G(d,p) level.

Quantum chemical descriptors were calculated within the conceptual framework of the DFT to determine the reactivity of drugs. The reactivity of molecules can be predicted with global descriptors, which are determined by perturbations related to the change in the number of electrons. Some of the global descriptors studied in this paper are chemical potential ( $\mu$ ), hardness ( $\eta$ ), electrophilic index ( $\omega$ ), and softness (S). Hardness, softness, and chemical potential were calculated by Koopman's theorem. According to this theorem ionization potential and electron affinity of a system are equal to the negative value of the energy of the highest occupied molecular orbital (E<sub>HO</sub>. MO) and the energy of the lowest unoccupied molecular orbital (E<sub>LUMO</sub>). By using the Koopman's theorem these global reactivity descriptors are defined as 36-38,

$$\mu = \frac{E_{LUMO} + E_{HOMO}}{2} \,, \tag{1}$$

$$\eta = \frac{E_{LUMO} - E_{HOMO}}{2} , \qquad (2)$$

$$\omega = \frac{\mu^2}{2\eta} \,, \tag{3}$$

$$S = \frac{1}{2n} \,, \tag{4}$$

#### 3. Results and Discussion

#### 3. 1. Energies and Global Descriptors

The structures of nine studied COVID-19 drugs, hydroxychloroquine, chloroquine, nitazoxanide, favipiravir, galidesivir, ribavirin, fluvoxamine, molnupiravir, and paxlovid, are shown in Figure 1 and optimized geometries of drugs are given in Figure 2. Some of these drugs are functionalized derivatives of the classic heteroaromatic rings, such as quinoline (hydroxychloroquine and chloroquine as molecules 1, 2), thiazolide (nitazoxanide as molecule 3), pyrazine (favipiravir as molecule 4). Others are nucleoside-based heterocyclic molecules, similar to the adenosine base of galidesivir (molecule 5) and the guanosine base of ribavirin (molecule 6). The newly proposed alter-

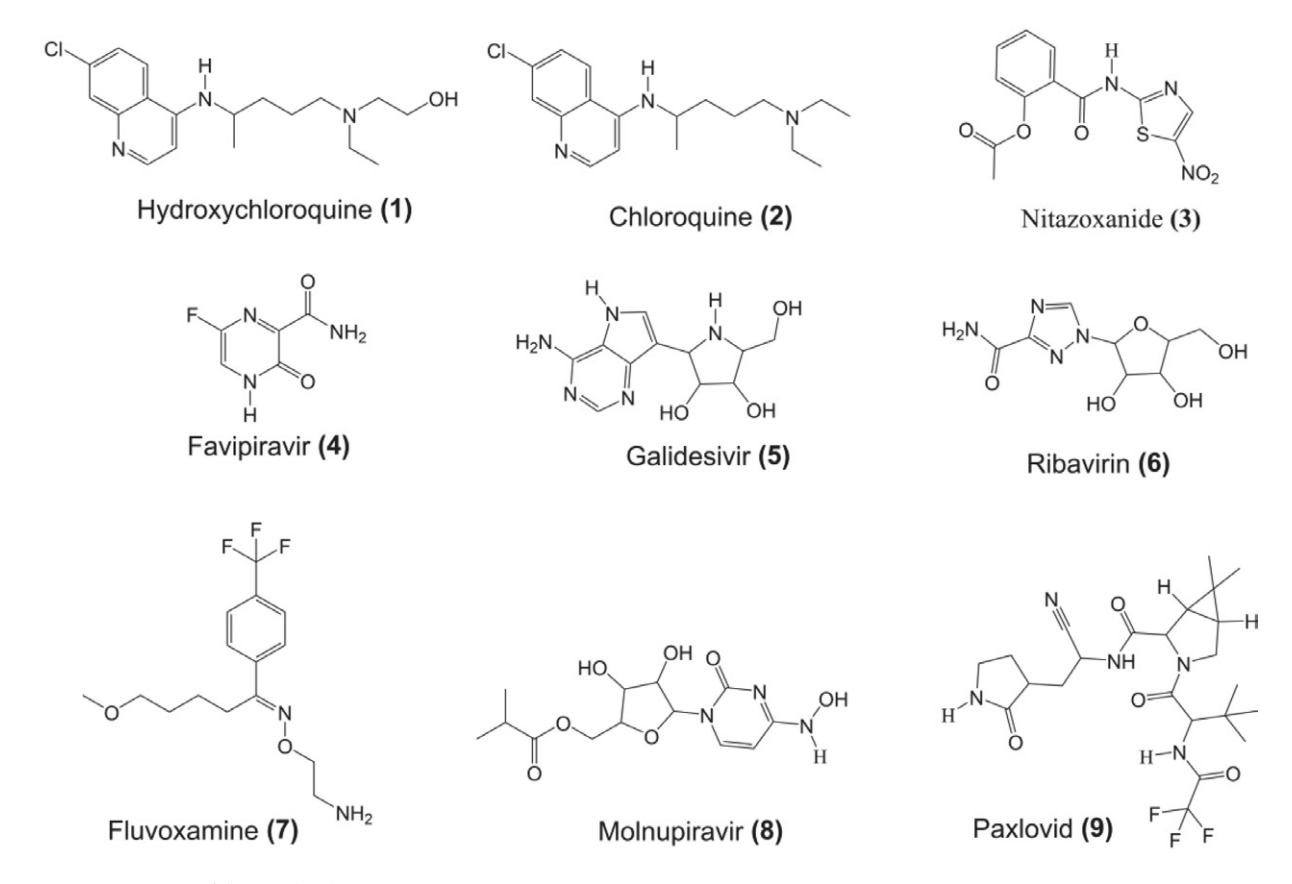


Figure 1. Structures of drug molecules

native drugs are fluvoxamine (molecule 7), a selective serotonin reuptake inhibitor (SSRI), ribonucleoside antiviral prodrug molnupiravir (molecule 8), and nitrile warhead paxlovid (molecule 9).

The calculated  $E_{HOMO}$ ,  $E_{LUMO}$ ,  $\Delta E$ , hardness ( $\eta$ ), chemical potential (μ), electrophilic index (ω), softness (S) and dipole moments (D) are listed in Table 1 for gas and aqueous media. The hardness is a good descriptor for chemical stability and reactivity and it is related to the energy gap. Hard molecules have large band gap energies. As seen in Table 1 the hardest molecules are 6 and 9, the least hard is 3. Molecules 5, 6, 7, 8, and 9, which contain electronegative atoms such as -OH and -F in their molecular structure, are those with highest hardness. Molecules 1, 2 and 3, which have fewer electronegative atoms in their molecular structure, are those with low hardness compared to the others. Molecule 3, which contains one sulfur atom in the ring in its structure, has the lowest hardness. The hardness of molecules increases in order of 6>9>7>5>8>4>1>2>3. Softness is the opposite of hardness, and posseses a similar relation. The chemical potential  $(\mu)$  is the measure of escaping tendency of electrons. The chemical potential also shows almost the same trend with hardness except for molecules 4, 5, and 8.

The electron accepting ability of a molecule is related to its electrophilicity index value. The electrophilic index

value of molecules is in order 4>3>1>6>2>8>7>9>5. Molecules with an electrophilic index value higher than 1.5 eV have an electrophilic character.<sup>37</sup> As seen in Table 1, the electrophilic index value of all drug molecules is greater than 1.5 eV. Therefore, it can be inferred that all the studied molecules have an electrophilic character. It is known that the cysteine moieties of proteins are nucleophilic. So, it is advantageous to have an electrophilic agent for the treatment of COVID-19.<sup>39</sup> In general, all drugs have in common the ability to accept electrons, which may increase the interaction of drugs with the SARS-COV-2 virus.

The in vitro half-maximal effective concentration ( $EC_{50}$ ) values for SARS-COV-2 virus in Vero E6 values are given in Figure 3. As can be seen in the figure, the molecules with the highest  $EC_{50}$  values are 6, 9, and 4, respectively. These drugs are less efficient than the others. Molecule 9, Paxlovid, is the new drug which Pfizer has developed for COVID-19 and has just been approved for use. Molecule 6, Ribavirin is in a class of antiviral medications, and molecule 4, Favipiravir, is the more efficient drug for COVID-19 disease. Favipiravir, as an antiviral drug, has been authorized for treating COVID-19 in several countries, under emergency provisions. There is a relationship between the  $EC_{50}$  values of the molecules and their global descriptors. Drugs with high  $EC_{50}$  values have high hardness and lower chemical potential values. Although there

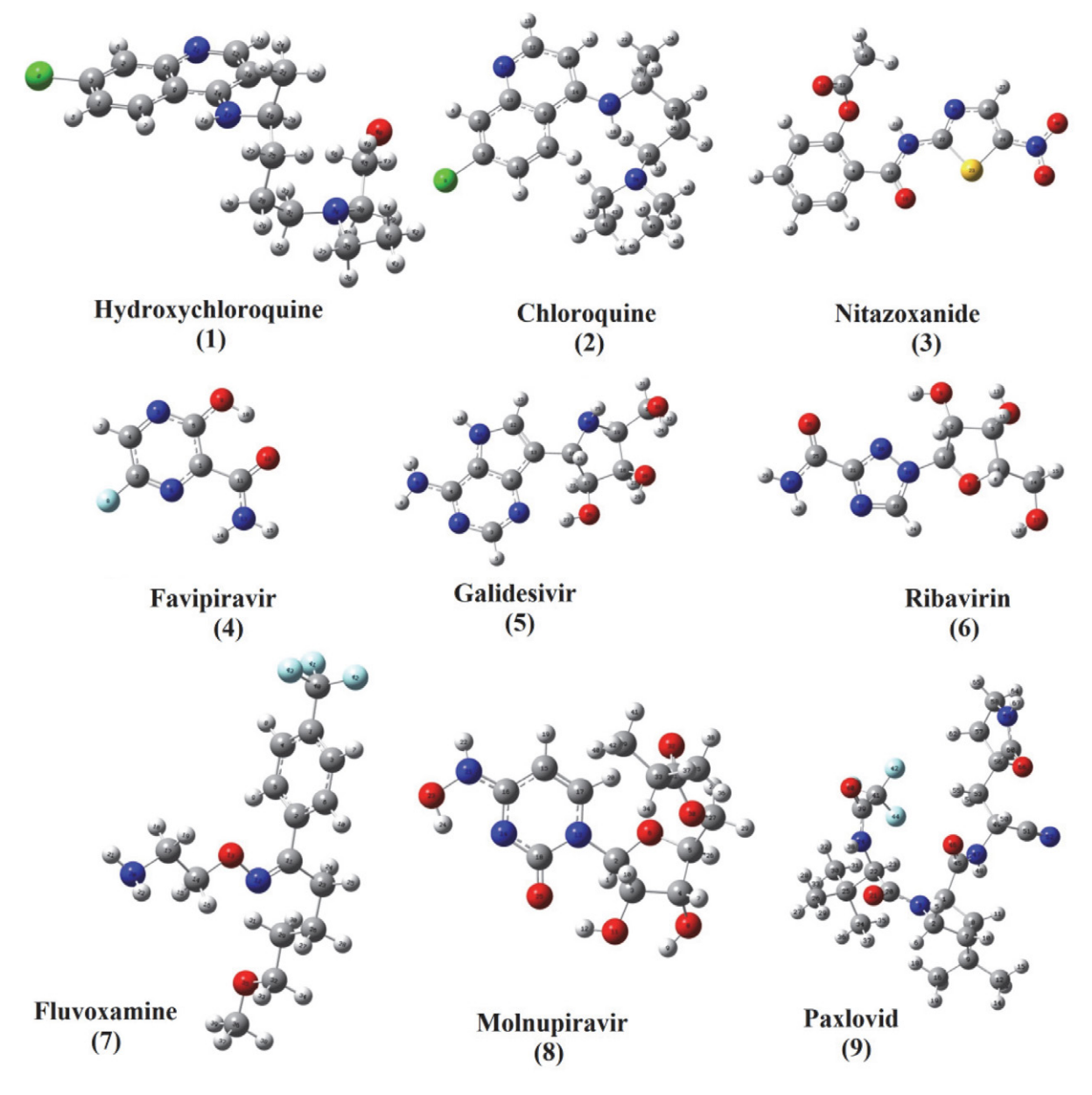


Figure 2. Optimized geometries of drug molecules

are not enough experimental studies on the efficacy of these drugs for COVID-19, the relationship between the global descriptors of these drugs and their  $EC_{50}$  values can be used to select the effective drug candidates.

The dipole moment is an important factor affecting the solubility of a drug. The solubility and polarity of the drug must be balanced to optimize the drug efficacy.<sup>3</sup> In biological systems, a high dipole moment value is a desirable property for drug delivery.<sup>16</sup> Dipole moments of drug molecules increase in the aqueous medium because of the hydrogen bonds. It means that the solubility of these drugs in an aqueous medium may be enhanced with the increase of polarity. The dipole moments of the molecules (1-9) are around 3.04–26.10 Debye in the aqueous

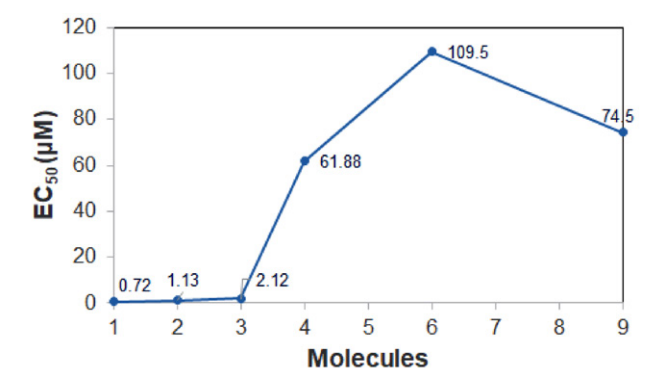


Figure 3. In vitro half-maximal effective concentration (EC $_{50}$ ) of drugs

**Table 1.** Global descriptors: hardness  $(\eta)$ , chemical potential  $(\mu)$ , electrophilic index  $(\omega)$ , softness (S), frontier orbitals energies  $(E_{HOMO}, E_{LUMO})$  and dipole moments (D) of drugs, (values in italic apply to the gas phase)

	E <sub>HOMO</sub> eV	E <sub>LUMO</sub> eV	ΔE eV	η eV	S eV	μ eV	ω eV	D Debye
1	-6.05	-1.71	4.34	2.17	0.23	-3.88	3.46	9.29
	-5.99	-1.59	4.40	2.20	0.23	-3.62	3.27	6.90
2	-5.94	-1.65	4.29	2.15	0.23	-3.80	3.36	9.26
	-5.81	-1.44	4.37	2.18	0.23	-3.62	3.01	6.99
3	-3.81	-2.00	1.81	0.91	0.55	-2.91	4.66	26.10
	-3.07	-0.82	2.25	1.12	0.44	-1.94	1.68	14.58
4	-7.31	-2.73	4.58	2.29	0.22	-5.02	5.50	4.31
	-7.37	-2.85	4.52	2.26	0.22	-5.11	5.77	3.24
5	-6.35	-1.20	5.15	2.57	0.19	-3.77	2.77	8.63
	-6.37	-1.31	5.05	2.53	0.20	-3.84	2.92	6.70
6	-7.75	-1.51	6.25	3.12	0.16	-4.63	3.43	3.04
	-7.45	-1.44	6.03	3.02	0.17	-4.46	3.30	2.08
7	-6.94	-1.41	5.53	2.77	0.18	-4.18	3.15	4.19
	-6.83	-1.64	5.19	2.60	0.19	-4.23	3.45	5.20
8	-6.66	-1.54	5.12	2.56	0.20	-4.10	3.29	6.41
	-6.71	-1.66	5.05	2.53	0.20	-4.19	3.47	5.20
9	-7.14	-1.13	6.01	3.00	0.17	-4.13	2.85	8.71
	-7.15	-0.94	6.22	3.11	0.16	-4.04	2.63	5.58

medium and 2.08–14.58 Debye in the gas phase. Among the calculated drug molecules the largest dipole moment value is found for molecule **3**. This large dipole moment value can allow high polarity in some regions of the drug

and hydrophilic interactions in the solvent that increases its activity. Dipole moments 1,2,5 and 9 are greater than those of 4,6,7 and 8. Hence, 1,2,5 and 9 are more polarized and may show more hydrophilic properties. This

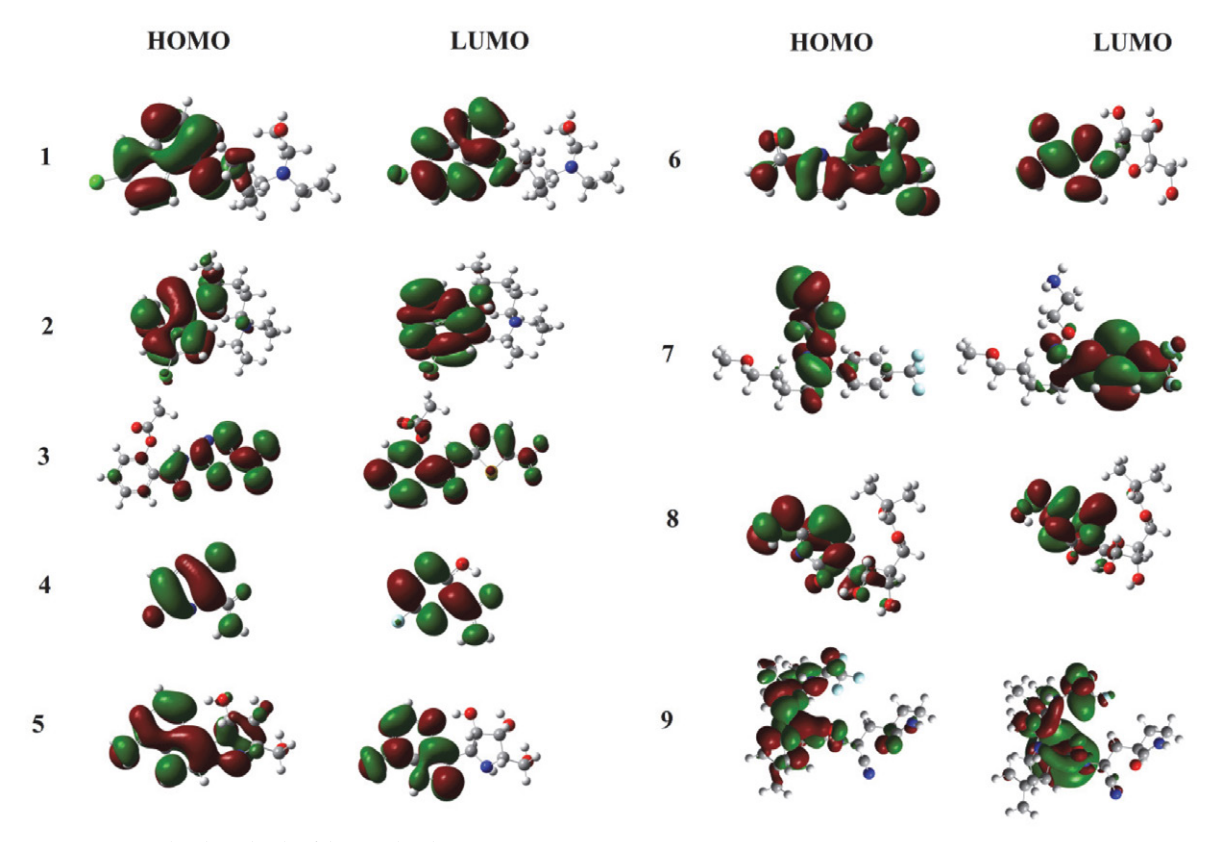


Figure 4 Frontier molecular orbitals of drug molecules

feature can turn these drugs into active molecules in an aqueous media.

#### 3. 2. Frontier Molecular Orbitals Analysis

Frontier Molecular Orbitals (FMOs) are important parameters used to understand the distribution of electrophilic regions of molecules and their chemical interaction parts with other molecules. The chemical reactivity of a molecule can be determined by using the energy gap value of frontier orbitals ( $\Delta E$ ). A small energy gap indicates a more reactive molecule. As seen in Table 1, molecule 3 has the smallest  $\Delta E$  values in both phases. Thus, this molecule is the most reactive one. The electron-withdrawing -NO<sub>2</sub> group in 3, can disrupt the distribution of the  $\pi$  electron

system, which leads to deteriorated molecular backbone conjugation, thus decreasing the chemical stability of the molecule. Molecule **6** is the least reactive molecule with the highest energy gap value of 6.25 eV.

The FMOs of all studied drug molecules are given in Figure 4. As can be seen from the Figure, the HOMO orbitals are  $\pi$ -bonding molecular orbitals. HOMO and LUMO orbitals are mainly distributed on the quinoline ring of the molecule for **1** and **2**. While HOMO of molecule **3** is distributed on the functionalized part of the thiazolidine ring, LUMO is distorded all through the molecule. The HOMO orbital is  $\pi$  bonding type and the LUMO orbital is  $\pi^*$  antibonding type for molecule **4** and they are mainly distributed all through the molecule. For molecules **5** and **6**, the electron distribution of the HOMO or

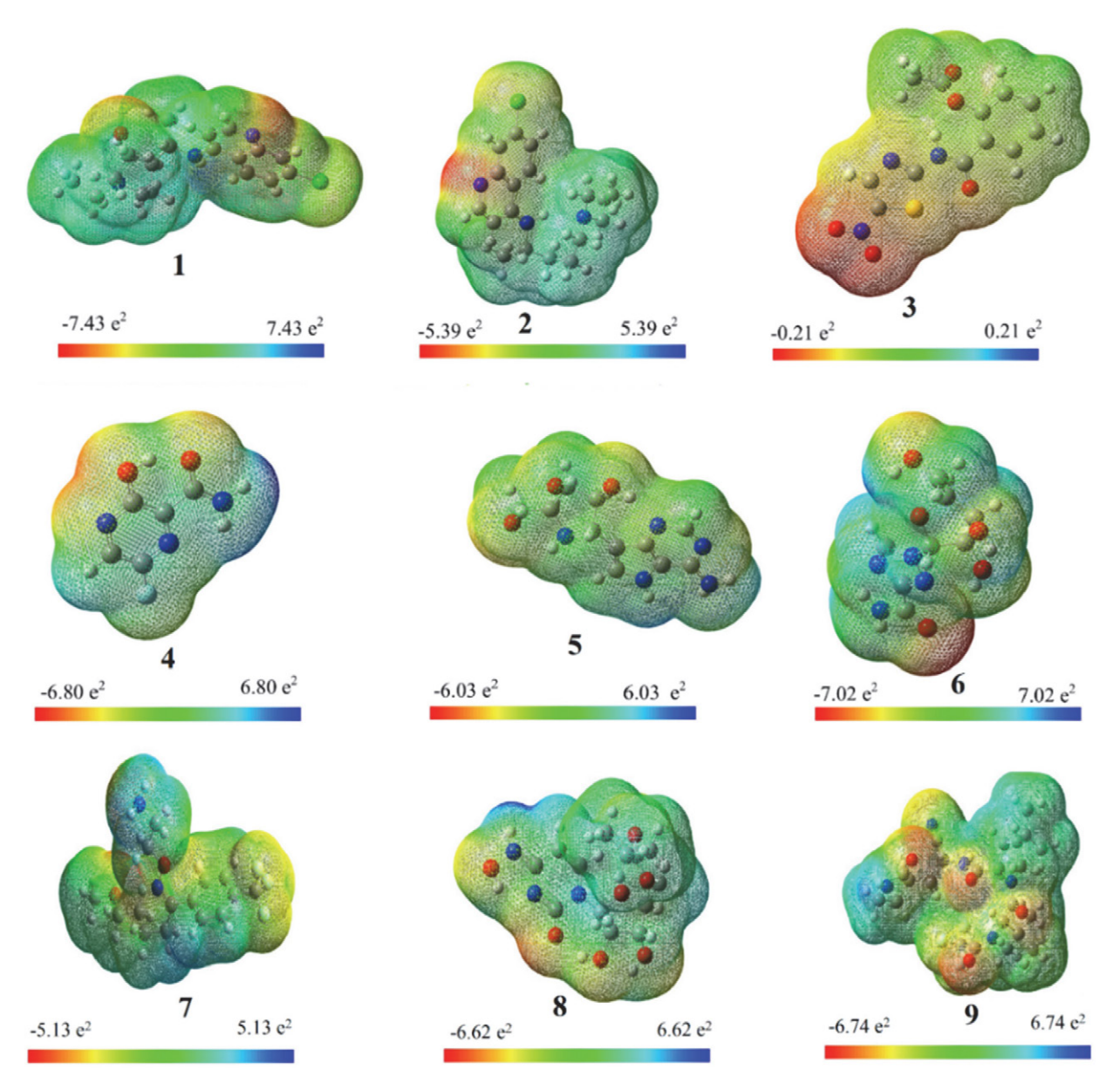


Figure 5. Molecular Electrostatic Potential Plots of molecules

bital is delocalized almost throughout the molecule, while the LUMO orbital is found in its two fused aromatic rings in molecule 5 and at the 1,2,4-triazole portion in molecule 6. HOMO is distributed on the etheric part and LUMO is on the benzene trifluoro acetamide part of molecule 7. The HOMO and LUMO orbitals of the antiviral prodrug 8 are distributed over the heterocyclic rings of the molecule. The boundary orbitals electron cloud is mainly on the pyrrolidine ring and isobutyl portion of molecule 9. In the study of Macchiagodena et.al., these parts of molecule 9 were found to approach to the SARS-COV-2 6LU7 protein.<sup>22</sup> Thus, according to FMOs, these sites are predicted as the active sites for the probable chemical interactions.

#### 3. 3 MEP Surfaces

Molecular Electrostatic Potential (MEP) surfaces are the three-dimensional visualization of the charge distribution of atoms on a molecule. Such surfaces supply information about electronic distribution of molecules, their nucleophilic and electrophilic attack parts, and formation of possible hydrogen bonds. In these surfaces, the red color shows the more negative potential of the molecule whereas the blue color shows the more positive potential. The green color represents the neutral part of the molecule with almost zero charge.

MEP surfaces of the molecules 1-9 are shown in Figure 5. For all molecules, at least one hydrogen bonding region is detected. Thus, hydrogen bonding stabilizations decrease the energy values of the molecules with the aqueous media.

As seen in Figure 5, the electron distributions of 1 and 2 are almost the same, but they differ in the number of hydroxyl groups. Since molecule 1 has more hydroxyl groups, its negative regions are dominant. Thereby, it is more effective against SARS-COV-2 than that of molecule 2.11,19,30 Molecule 3 has more red areas than the others, and they are mainly concentrated on the -NO<sub>2</sub> group, which removes the electron density from the molecule's  $\pi$  system and makes the molecule less electrophilic. The electrophilic region of molecule 4 is on the hydroxyl group while the hydrogen atoms of the amino group are the nucleophilic part. But the fluorine atom in 4 has no effect on the electronic behavior of the pyrazine ring. In molecule 5, the ribose ring has a higher electron density due to the electron-donating hydroxyl groups, while the electron-positive areas are hydrogens bonding to the nitrogen atom. In molecule 6, the most negative region belongs to the oxygen atom of the carbonyl group, and the positive potential region belongs to the hydrogen atoms. For molecule 7, the electrophilic regions are etheric oxygen and fluorine atoms. In molecule 8, the blue color distribution is in the hydrogen atoms of the amine group. Due to the electron withdrawal properties of fluorine atoms, this region in molecule 9 can cause electron localization.

#### 3. 4. Thermodynamic Properties

The solvatation-free energies of the studied drug molecules are calculated using their Gibbs free energy change values between the solvent phase and the gas phase (Figure 6). As depicted from the figure, all the molecules' solvation-free energies are negative, indicating their spontaneous solubility in water. This result is in accordance with the increased dipole moment values in the aqueous medium. The solvation energies of the molecules vary between (-6.83) – (-53.99) kcal mol<sup>-1</sup>. As noticed in Figure 6, the solvation free energies of all molecules, are quite similar except of molecule 3. Since molecule 3 has less electronegative atoms in its structure, it differs from the others. Molecules 1 and 2, 4, and 7 are structurally very similar. Therefore their solvation-free energies are also close to each other, for 1 and 2 they are -8.66, -6.83 kcal  $\text{mol}^{-1}$  and for 4 and 7 -8.15, -9.14 kcal  $\text{mol}^{-1}$  respectively. For molecules 5, 6, 8, 9 solvation-free energies are found as -14.48, -13.81, -16.31 and -18.72 kcal mol<sup>-1</sup>, respectively.

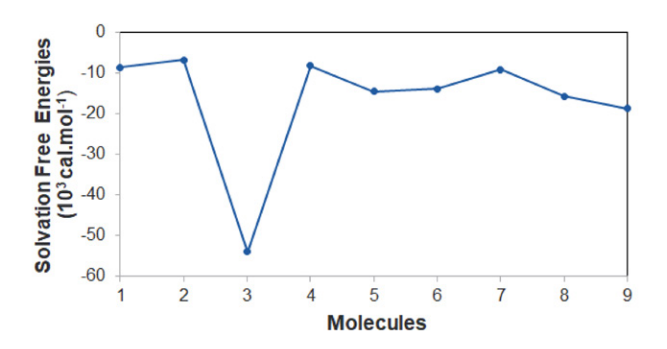


Figure 6. Solvation-free energies of drugs

Thermodynamic parameters of the studied drug molecules have been calculated at 298.15 K. The calculated total energies (E), enthalpy ( $\Delta$ H), entropy (S), Gibbs free energy ( $\Delta$ G) with ZPE correction for water and gas phases are listed in Table 2. As can be seen from the table, the molecules with the lowest energies are 9, 3, and 1, while the molecules with the highest energies are 4, 6, and 5. The most thermodynamically stable molecules are found as 9, 3, and 1 due to their enthalpy and Gibbs free energy values (Table 2). The thermal stabilities of all molecules are higher in the aqueous medium. Since the thermal stability of drug molecules is necessary for drug durability, it can be inferred from the results that all molecules are more stable in an aqueous medium. <sup>46</sup>

# 3. 5. The Effect of Electronic Structure on Biological Effectiveness

A drug binding efficiency to an active point of an enzyme or a protein is related to its electronic structure.<sup>47</sup> Therefore, the electronic properties of drugs are important

	1	2	3	4	5	6	7	8	9	
Aqueous medium										
$\angle ZPE.10^6$	0.26	0.26	0.13	0.06	0.18	0.14	0.22	0.21	0.34	
$E.10^{6}$	-879.21	-832.00	-879.41	-381.27	-582.10	-569.30	-717.64	-751.54	-1110.63	
$\Delta H . 10^6$	-879.20	-831.99	-879.40	-381.26	-582.09	-569.30	-717.63	-751.52	-1110.61	
$\Delta G . 10^6$	-879.25	-832.03	-879.44	-381.30	-582.13	-569.33	-717.68	-751.57	-1110.67	
S	163.53	160.47	146.88	92.70	132.54	127.72	176.80	165.37	220.36	
Gas										
$ZPE.10^6$	0.26	0.26	0.13	0.06	0.18	0.14	0.22	0.21	0.35	
$E.10^{6}$	-879.21	-831.99	-879.32	-381.26	-582.09	-569.29	-717.64	-751.52	-1110.61	
$\Delta H . 10^6$	-879.19	-831.98	-879.31	-381.26	-582.08	-569.28	-717.62	-751.50	-1110.58	
$\Delta G . 10^6$	-879.21	-832.03	-879.35	-381.28	-582.12	-569.32	-717.68	-751.55	-1110.65	
S	169.13	159.39	148.30	92.02	128.92	130.39	177.00	162.18	232.45	

Table 2. Calculated energies and thermodynamic parameters of drugs. ZPE, E, ΔH, ΔG (in cal.mol<sup>-1</sup>), S (in cal mol<sup>-1</sup> K<sup>-1</sup>)

for predicting their biological activity. In Figure 3, the in vitro half-maximal effective concentration (EC<sub>50</sub>) values of molecules are shown for the studied molecules except for 5, 7, and 8.<sup>7,12,48</sup>

According to the results of experimental biological studies, it was understood that quinoline derivative drugs 1 and 2 in Vero E6 were more active for the SARS-COV-2 virus. Because the unpaired electrons of the nitrogen atom in the quinoline ring and the availability of suitable sites for the hydrogen bond affect the activities of these types of drugs positively. 49,50 The reason why the EC<sub>50</sub> value of 1 is less than that of 2 may be due to the hydrogen bonding of the hydroxyl group in its structure. Molecule 3 may be an important molecule to treat COVID-19 due to the presence of sulfur atom in its structure, which may change the amino acid residue of the target compound by disulfide bond formation. In addition, the sulfur atom may be important for the formation of a hydrogen bond.<sup>51</sup> However, the electron-withdrawing feature of the -NO2 group in the structure of 3 reduces the electron conjugation, resulting in a higher  $EC_{50}$  value than for 1 and 2. The lone pair electrons, halogen atom, and electron conjugation of the heterocyclic ring make molecule 4 more effective than molecule 6 against COVID-19 disease. It is known that halogen atoms increase the electron density of the rings for  $\pi$ -stacking interactions as well as halogen bonding.<sup>44</sup> It is understood from the results of the Saul et al. study<sup>8</sup> that 1 and 2 are more effective against COVID-19 than 4. The decreased electronegativity of the halogen atom in drugs 1 and 2 can increase the electron density of the quinoline ring, which may lead to the interaction of these molecules with the target site of SARS-COV-2. Altough molecule 6 has a lower conjugate electron cloud in its structure, its highest hydrogen bonding ability causes an easier to attach to the target site in comparison to the other molecules. The trifluoroacetamide moiety of molecule 9 is the potential site for hydrogen bond interactions with the amino acid of the spike protein. The halogen-type hydrogen bonding ability and electron-withdrawing substituents are key factors governing the biological effectiveness. Based on all these results, we can say that the structural modification of drugs has a significant effect on the electronic structure of drugs. Therefore, a complete characterization of the electronic properties of drugs is important to understand their biological activities.

#### 4. Conclusions

The fight against COVID-19 can be achieved with both vaccine prevention and drug treatment. Electronic behavior of drugs may point out their effectiveness against genetic variants of SARS-COV-2. In this study, electronic and thermodynamic properties, and quantum chemical descriptors of nine drugs are calculated. The results can be summarized as follows:

- Drug molecules containing electronegative atoms such as -OH and halogen atoms have higher hardness. Molecule 6 (ribavirin) is found as the hardest molecule.
- Electrophilic character of drug molecules may increase their interaction with SARS-COV-2.
- Paxlovid (9), nitazoxanide (3), and hydroxychloroquine (1) are found as the most thermodynamically stable drug molecules. All the studied molecules are thermodynamically more stable in an aqueous medium.
- The trifluoroacetamide in molecule 9 may be the appropriate site for binding to the amino acid of the spike protein.
- Structures of drugs have a significant effect on their electronic properties. Accordingly, their biological activities may also differ.
- The frontier molecular orbitals and MEP surfaces allow the prediction of reactive and possible interaction sites of drug molecules. Nucleophilic attacks may take place to the quinoline ring, two fused heterocyclic ring of 1 and 2, 1,2,4-triazole

parts of **6**, and pyrrolidine ring, isobutyl part of the **9** 

In summary, quantum chemical descriptors and electronic properties can be used as suitable parameters to evaluate the efficacy of drugs to treat COVID-19.

#### Acknowledgements

The authors express their thanks to Yildiz Technical University. Project No. 2012-01-02-KAP02

#### 5. References

- A. Hazafa, F. Abbas, S. Bano, M. Farman, N. Jahan, M. Mumtaz, H. Naeem, M. Naeem, S. Sadiqa, I. ul- Haq, K. ur-Rahman, *Drug Metab Rev*, 2020, 52 (3), 408–424.
   DOI:10.1080/03602532.2020.1770782
- D. L. McKee, S. Laufer, C. Naujokat, U. Stange, A. Sternberg, *Pharmacol Res*, **2020**, *157*, 104859-104868.
   DOI:10.1016/j.phrs.2020.104859
- 3. V. V. Kouznetsov, Eur J Med Chem, 2020 203 (112647), 1-10.
- C. Ma, Y. Chen, Y. Hu, B. Hurst, M.T. Marty, M.D. Sacco, T. Szeto, B. Tarbet, J. A. Townsend, J. Wang, X. Zhang, Cell Res, 2020, 30, 678–692. DOI:10.1038/s41422-020-0356-z
- 5. J. Shio-Shin, L. Ping-Ing, H. Po-Ren, *J Microbiol Immunol Infect*, **2020**, *53*, 436–443.
- WHO (2021), Official Updates Coronavirus Disease 2020, Coronavirus disease (COVID-19) pandemic website, https:// www.who.int/emergencies/diseases/novel-coronavirus-201 accesed time 31.01.2022
- J. Zhe, L. Hai-Bo, L. Jing-Yi, J. Lu, F. Rang, J. Zi-Li, Eur J Pharmacol, 2020, 883, 173326–173333.
- S. Saul, S. Einav, ACS Infect. Dis 2020, 6, 2304–2318.
   DOI:10.1021/acsinfecdis.0c00343
- P. M. Mitrasinovic, Acta Chim. Slov. 2020, 67, 949–956
   DOI:10.17344/acsi.2020.6009
- B. Furlani, K Kouter, D. Rozman, A. V. Paska, *Acta Chim. Slov.* 2021, 68, 268–278 DOI:10.17344/acsi.2021.6691
- P. Chibber, A. S. Haq, I. Ahmed, N. I. Andrabi, G. Singh, Eur J Pharmacol, 2020, 883, 173372–173387.
  - **DOI:**10.1016/j.ejphar.2020.173372
- M. Wang, R. Cao, Z. Hu, J. Liu, Z. Shi, G. Xiao, M. Xu, X. Yang, L. Zhang, W. Zhong, Cell Res, 2020, 30, 269–271.
   DOI:10.1038/s41422-020-0282-0
- E. A. Coomes, H. Haghbayan, J Antimicrob Chemother, 2020, 75, 2013–2014. DOI:10.1093/jac/dkaa171
- 14. H. Koba, K. Kasahara, H. Kimura, T. Kaneda, T. Ueda, T. Yoneda, *Clin Case Rep* **2020**, *00*, 1–6.
- 15. WHO Coronavirus disease (COVID-19): Vaccines https://ourworldindata.org/covid-vaccinations (accessed time 27.12.2021)
- S. G. Novir, M.R. Aram, Chem Phys Lett, 2020, 757 (137869),
   1–10. DOI:10.1016/j.cplett.2020.137869
- 17. N. Al-Masoudi, R.S. Elias, B. Saeed, *Biointerface Res Appl Chem*, **2020**, *10* (5), 6444–6459

#### DOI:10.33263/BRIAC105.64446459

- L. I. Hage-Melim, M.P. Barcelosb, L.C. Correia, H.B. de Lima, N. K. S. de Oliveiraa, C. H. T. de Paula da Silva, L. B. Federico, V. C. C. Franciscoa, I. A. G. Francischini, S. Q. Gomes, *Life Sci*, 2020, 256 (117963), 1–13. DOI:10.1016/j.lfs.2020.117963
- 19. D. Gentile, V. Fuochi, P.M. Furneri, A. Rescifina, *Int J Mol Sci*, **2020**, *21* (5856), 2–16. **DOI:**10.3390/ijms21165856
- 20. B. Ahmad, M. Batool, Q. Ain, M. S.Kim, S. Choi, Exploring the Binding Mechanism of PF-07321332 SARS-CoV-2Protease Inhibitor through Molecular Dynamics and Binding Free Energy Simulations *Int. J. Mol. Sci.*, **2021**, *22*, 2–13. **DOI:**10.3390/ijms22179124
- M. Pavan, G. Bolcato, D. Bassani, M. Sturlese, *J Enzyme Inhib*,
   2021, 36 (1), 1646–1650.
   DOI:10.1080/14756366.2021.1954919
- M.Macchiagodena, M.Pagliai, P. Procacci, J. Mol. Graph. 2022, 110, 108042–108051. DOI:10.1016/j.jmgm.2021.108042
- M. Jukič, K. Kores, D. Janežič, U. Bren, Front. Chem. 2021, 9, 757826. DOI:10.3389/fchem.2021.757826
- M. Jukic, D. Janežic, U. Bren, *Int. J. Mol. Sci.* 2021, 22, 11143.
   DOI:10.3390/ijms222011143
- M. Jukic, D. Janežic, U. Bren, *Molecules* 2020, 25, 5808.
   DOI:10.3390/molecules25245808
- M. Jukic, B. Škrlj, G.r Tomšic, S. Pleško, C. Podlipnik, U. Bren, *Molecules*, 2021, 26, 3003. DOI:10.3390/molecules26103003
- A. V. Sharov, T. M. Burkhanova, T. T. Tok, M. G. Babashkina,
   D. A. Safin, *Int. J. Mol. Sci.* 2022, 23, 1508.
   DOI:10.3390/ijms23031508
- T. da S. Arouche, A. F. Reis, A. Y. Martins, J. F. S. Costa, R. N. C. Junior, A. M. J. C. Neto, J. Nanosci. *Nanotechnol.*, 2020, 20, 7311–7323. DOI:10.1166/jnn.2020.18955
- Ö. Alver, C. Parlak, P. Ramasami, Y. Umar, Main Group Met Chem, 2019, 42, 143–149. DOI:10.1515/mgmc-2019-0016
- G. W. Ejuh, C. Fonkem, J. M. B. Ndjaka, L. P. Ndukum, T. Nya, Y. Tadjouteu Assatse, R. A. Yossa Kamsi, *Heliyon*, 2020, 6 (04647), 1–11. DOI:10.1016/j.heliyon.2020.e04647
- T. A. Altalhi, K. Alswat, W. F. Alsanie, A. Aldalbahi, H. S. El-Sheshtawy, M. M. Ibrahim, *J. Mol. Struct*, 2021, 1228, 129459–129468. DOI:10.1016/j.molstruc.2020.129459
- M. J. Frisch, C. Adamo, A.J. Austin, et al. 2009 Gaussian 09 Revision B.01. Gaussian Inc., Wallingford
- 33. L. Rhyman, H. H. Abdallah, Y. S. Choong, P. Kharkar, C. Parlak, P. Ramasami, M. Tursun, *Phys Sci Rev*, **2018**, *20170198*, 1–10.
- R. Dennington, T. Keith, J. Millam GaussView, Version 5, Semichem Inc., Shawnee Mission, KS, 2009
- J. Foresman, E. Frish Exploring chemistry. 1996 Gaussian Inc, Pittsburg
- P. Geerlings, F. De Proft, W. Langenaeker, *Chem Rev*, 2003, 103, 1793–1874. DOI:10.1021/cr990029p
- L. R. Domingo, P. Perez, Org Biomol Chem, 2011, 9, 7168–7175. DOI:10.1039/c1ob05856h
- C. Soriano-Correa, C. Barrientos-Salcedo, R. O. Esquivel, A. Raya, *Chem Phys* **2014**, *438*, 48–59.
   DOI:10.1016/j.chemphys.2014.04.012
- 39. S.Ray, A. S.Murkin, Biochemistry, 2019, 58, 5234-5244.

- DOI:10.1021/acs.biochem.9b00293
- 40. L. Chih-Chia, C. Mei-Yu, L. Wan-Shin, C. Yuh-Lih, J Chin Med Assoc, 2020, 83 (6), 534-536.
- 41. G. W. Ejuh, J. M. B. Ndjaka, Y. T. Assatse, C. Fonkem, R. A. Y. Kamsi, P. L. Ndukum, F. T. Nya, Opt Quantum Electron, 2020, 52, 498, 1-22. **DOI:**10.1007/s11082-020-02617-w
- 42. L. H. M. Huziar, N. J. Olvera-Maturana, C. H. Rios-Reyes, J. Robles, J. A. Rodriguez, Open Chem, 2015, 13, 52-60.
- 43. N. Sepay, U. C. Halder, A. A. Hoque, R. Mondal, M. Muddassir, N. Sepay, Struct Chem, 2020, 31, 1831-1840. DOI:10.1007/s11224-020-01537-5
- 44. A. Sagaama, S. Antonia Brandan, T. B. Issa, N. Issaoui, Heliyon, 2020, 6 (e04640) 1-29.
  - DOI:10.1016/j.heliyon.2020.e04640

- 45. J. S. Al- Otaibi, Spectrochim Acta A, 2020, 235 (118333), 1-5. DOI:10.1016/j.saa.2020.118333
- 46. H. Nikoofard, F. Faridbod, M. Sargolzaei, Acta Chim Slov, 2017, 64, 842-848. DOI:10.17344/acsi.2017.3357
- 47. S. M. LaPointe, D. F. A. Weaver, Curr Comput Aided Drug Des, **2007,** 3 (4), 290–296. **DOI:**10.2174/157340907782799390
- 48. J. Xu, H. Li, P. Y. Shi, J. Zhou, Broad Spectrum Antiviral Agent Niclosamide and Its Therapeutic Potential, ACS Infect Dis, **2020,** 6, 909–915. **DOI:**10.1021/acsinfecdis.0c00052
- 49. A. Ghaleb, A .Aouidate, M. Aarjane, H. Anane, H. B. El Ayouchia S. E. Stiriba, J Biomol Struct Dyn, 2020, 17, 1-11.
- 50. M. Hagar, H. A. Ahmed, G. Aljohani, O. A. Alhaddad, Int J. Mol Sci, 2020, 21 (3922), 1-13. DOI:10.3390/ijms21113922
- 51. S. Shekh, K. H. Gowd, A. K. K. Reddy, J Sulfur Chem, 2020, 42 (1), 1-12. **DOI:**10.1080/17415993.2020.1817457

#### **Povzetek**

Te dni se svet sooča z grožnjo pandemije koronavirusne bolezni 2019 (COVID-19). Čeprav je bilo najdeno cepivo za boj proti tej pandemični bolezni, je nujno, da čim prej poiščemo tudi zdravila za učinkovito metodo njenega zdravljenja. V tej študiji smo raziskali elektronske in termodinamične lastnosti in mejne molekularne orbitale (FMO) devetih različnih covidnih zdravil s teorijo gostotnega funkcionala (DFT) in z analizo molekularnega elektrostatičnega potenciala (EMP). Poleg tega smo preučili povezavo med elektronskimi strukturami teh zdravil in njihovo biološko učinkovitost. Vse parametre smo izračunali na ravni B3LYP/6-311+g(d,p). Vpliv topila smo ovrednotili z uporabo modela polarizirajočega kontinuuma (CPCM) kot modela solvatacije. Opazili smo, da so za razumevanje učinkovitosti teh zdravil pri bolezni COVID-19 pomembni elektrofilni indeksi. Paxlovid, hidroksikinon in nitazoksanid so se izkazali za najbolj termodinamično stabilne molekule. Termodinamični parametri so tudi pokazali, da so bila ta zdravila stabilnejša v vodnih medijih. Ugotovili smo, da so globalni deskriptorji in reaktivnost teh zdravil povezani. Molekula nitazoksanida je imela največji dipolni moment. Visoki dipolni momenti zdravil lahko povzročijo hidrofilne interakcije, ki povečujejo njihovo učinkovitost v vodni raztopini.



Except when otherwise noted, articles in this journal are published under the terms and conditions of the Creative Commons Attribution 4.0 International License